



## Fatigue crack tip damaging micromechanisms in a ferritic-pearlitic ductile cast iron

Francesco Iacoviello, Vittorio Di Cocco

*Università di Cassino e del Lazio Meridionale, DICeM, via G. Di Biasio 43, 03043 Cassino (FR), Italy*  
*iacoviello@unicas.it, v.dicocco@unicas.it*

Mauro Cavallini

*Università di Roma "Sapienza", DICMA, via Eudossiana 18, Rome, Italy*  
*mauro.cavallini@uniroma1.it*

---

**ABSTRACT.** Due to the peculiar graphite elements shape, obtained by means of a chemical composition control (mainly small addition of elements like Mg, Ca or Ce), Ductile Cast Irons (DCIs) are able to offer the good castability of gray irons with the high mechanical properties of irons (first of all, toughness). This interesting properties combination can be improved both by means of the chemical composition control and by means of different heat treatments (e.g. annealing, normalizing, quenching, austempering etc). In this work, fatigue crack tip damaging micromechanisms in a ferritic-pearlitic DCI were investigated by means of scanning electron microscope observations performed on a lateral surface of Compact Type (CT) specimens during the fatigue crack propagation test (step by step procedure), performed according to the "load shedding procedure". On the basis of the experimental results, different fatigue damaging micromechanisms were identified, both in the graphite nodules and in the ferritic – pearlitic matrix.

**KEYWORDS.** Ferritic-pearlitic ductile cast irons; Fatigue damaging mechanism; Crack tip.

---

### INTRODUCTION

**D**uctile iron discovery in 1948 gave a new lease on life to the cast iron family. In fact, these cast irons (DCIs) combine the good castability of gray irons and high toughness values of steels and they are also characterized by an interesting fatigue crack propagation resistance. Considering their interesting mechanical properties, DCIs are widely used in the critical automotive parts (e.g., crankshafts, truck axles, etc.), and in many other application, like pumps, pipes or turbine components [1, 2]. DCIs can be considered as natural composites, with graphite nodules embedded in a metal matrix. The DCIs performances are strongly affected by the graphite elements morphological peculiarities (e.g., graphite elements nodularity, volume fraction, density, distribution, dimension).

Different combinations of the mechanical properties can be obtained depending on the matrix microstructure [3]: ranging from ferritic to pearlitic DCIs, different combination of ductility or tensile strength values can be obtained (anyway, equivalent to the values offered by low carbon steels); martensitic DCIs are characterized by a very high strength, but low levels of toughness and ductility; bainitic grades are characterized by a high hardness; austenitic DCIs show good corrosion resistance, good strength and dimensional stability at high temperature; finally, austempered grades (ADI) show

---

a very high wear resistance and fatigue strength. Difference between DCIs and low carbon steels tensile properties are summarized in Fig. 1, considering the microstructure influence on UTS and elongation [4].

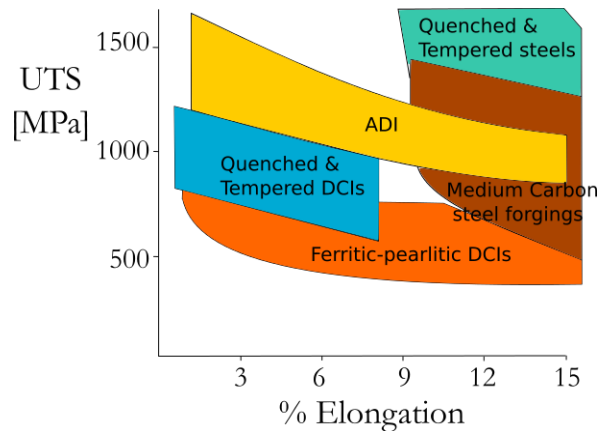


Figure 1: UTS-Elongation for different DCI and low carbon alloys [4].

Focusing on the fatigue crack propagation resistance, microstructure influence is more evident corresponding to higher values of the stress ratio and the applied stress intensity values [5], Fig. 2, where ferritic-pearlitic DCI (50% F – 50% P) shows a fatigue crack propagation resistance that is analogous to the investigated ADI. Cavallini et alii [5, 6] proposed that this behaviour is due to an enhanced crack closure effect, due to the graphite nodule presence and to the different phases distribution and mechanical properties. Considering that pearlite (or bainite, in ADI) is characterized by a reduced ductility and higher UTS (Ultimate tensile strength) values, if compared to ferrite, this second peculiar crack damaging mechanism can be described as follows (Fig. 3):

- corresponding to  $K_{max}$  values, ferritic shields are more deformed than pearlitic (or bainitic in ADI) matrix (considering an equivalent stress level);
- corresponding to  $K_{min}$  values, pearlitic (or bainitic in ADI) matrix induces on ferritic shields a residual compression stress condition with a consequent enhancing of the closure effect.

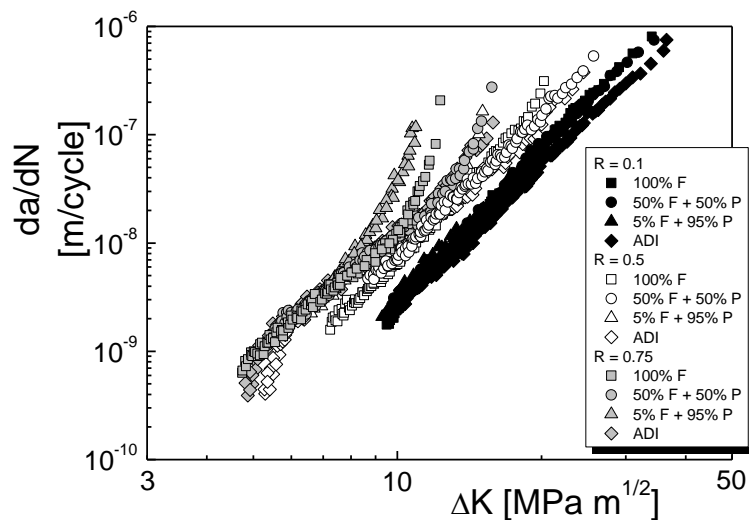


Figure 2: Microstructure and stress ratio influence on fatigue crack propagation in DCIs [5].

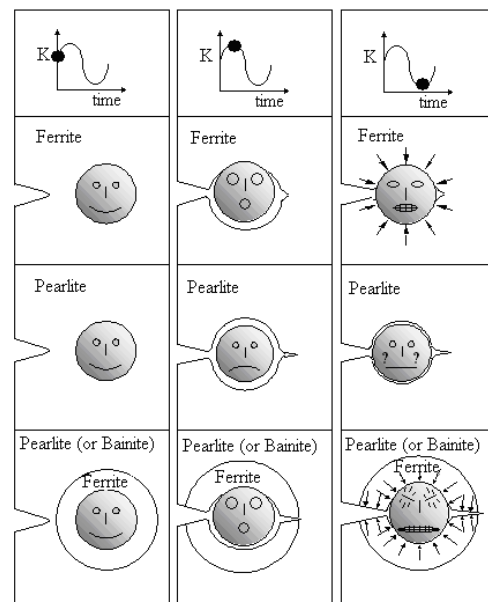


Figure 3: Ductile and fragile graphite elements debonding influence on crack closure effect in ductile irons [5].

In this work, fatigue crack tip damaging micromechanisms in a ferritic-pearlitic DCI were investigated by means of scanning electron microscope (SEM) observations of the lateral surface of metallographically prepared Compact Type (CT) specimens, focusing both the role played by the graphite nodules and the influence of the phases distribution.

## INVESTIGATED MATERIAL AND EXPERIMENTAL PROCEDURE

As cast ferritic – pearlitic DCI, with analogous ferrite and pearlite volume fraction and showing a peculiar “bull’s eye” morphology (Fig. 4) and characterized by a high graphite elements nodularity, were considered (chemical composition is shown in Tab. 1).

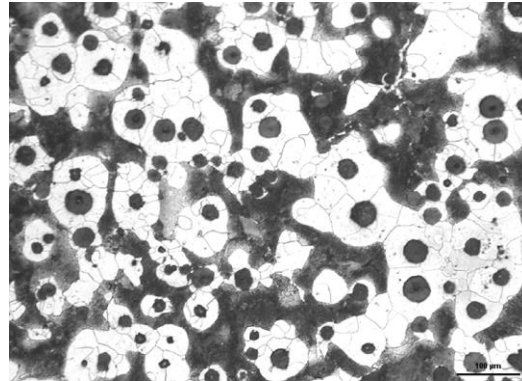


Figure 4: Investigated ferritic-pearlitic ductile iron: phases distribution (obtained by means of chemical composition control; Nital 3).

C	Si	Mn	S	P	Cr	Mg	Sn
3.65	2.72	0.18	0.010	0.03	0.05	0.055	0.035

Table 1: Investigated ferritic-pearlitic DCI chemical composition.

10 mm thick CT specimens were metallographically prepared and etched (Nital 3), and fatigue crack propagation tests were run according to ASTM E647 standard [7], considering one stress ratio value (e.g.  $R = P_{\min}/P_{\max} = 0.1$ ). Tests were performed using a computer controlled servohydraulic machine in load controlled conditions, considering a 20 Hz loading frequency, a sinusoidal loading waveform and laboratory conditions. Crack length measurements were performed by means of a compliance method using a double cantilever mouth gage and controlled using an optical microscope (x40). After the precracking procedure (measured crack length equal to 3 mm) a decreasing  $\Delta K$  values were applied according to the relationship:

$$\Delta K = \Delta K_0 e^{[C(a-a_0)]} \quad (1)$$

where  $\Delta K_0$  is the initial  $\Delta K$  at the beginning of the test (20 MPa $\sqrt{m}$ ),  $a_0$  is the corresponding crack length,  $a$  is the crack length during the test and  $C$  is equal to -0.291.

This procedure allowed to obtain a propagating crack with a decreasing crack tip plastic zone radius, up to threshold conditions (about 8 MPa $\sqrt{m}$ ), corresponding to a negligible crack tip plastic zone.

During the fatigue crack propagation tests, SEM crack path observations were performed with a step by step procedure. Furthermore, fracture surfaces were analysed by means of a scanning electron microscope, focusing both the graphite nodules and the metal matrix.

## RESULTS AND COMMENTS

Fatigue crack path is microscopically tortuous (Fig. 5a). This behaviour and the consequent fracture surface roughness were already extensively investigated [8, 9]: this parameter increases with the increase of the applied  $\Delta K$ . Superposing white spots to the fatigue crack path corresponding to the intersections between the crack path and the graphite nodules (Fig. 5b), it is evident that crack path tortuosity is strongly affected by the graphite nodules distributions: graphite nodules are not mere voids embedded in the metal matrix but they influence the crack path increasing the fracture surface roughness and, consequently, the importance of the roughness induced crack closure effect [10].

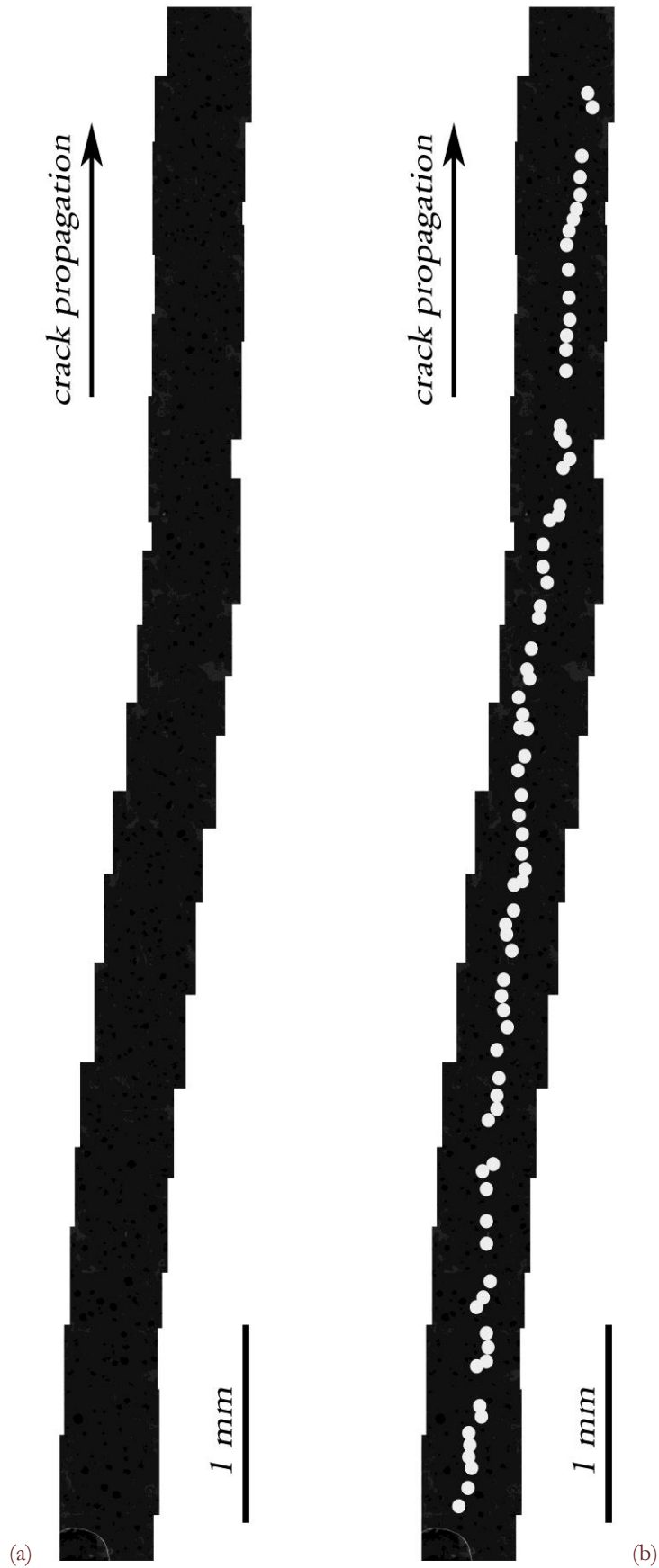


Figure 5: (a) Fatigue crack path; (b) fatigue crack path intersections with graphite nodules (with or without crack path deviations).

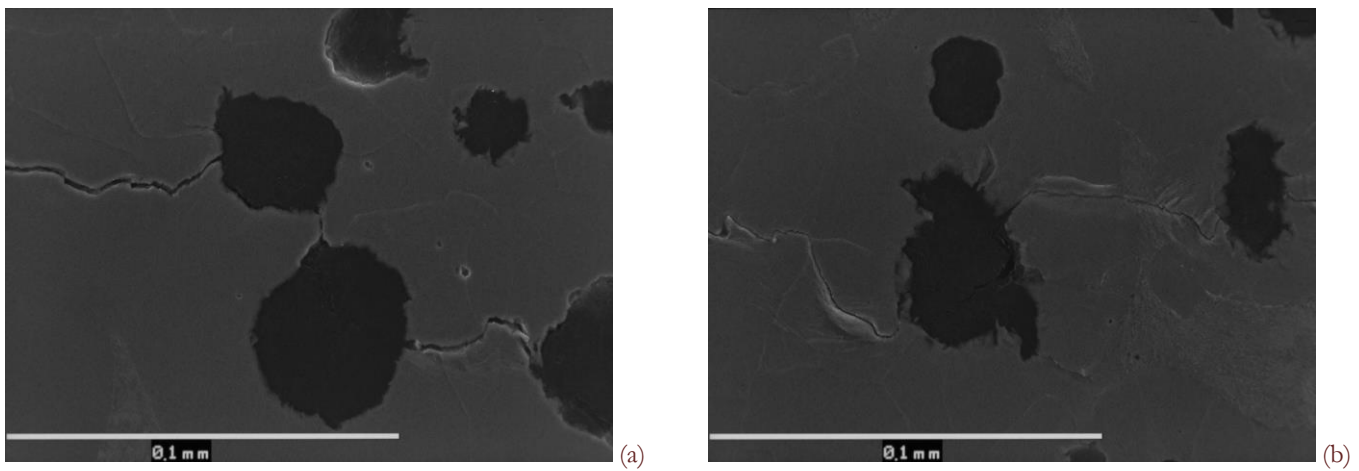


Figure 6: Fatigue crack path deviations corresponding to graphite nodules (crack grows from left to right). (a)  $\Delta K = 15 \text{ MPa}\sqrt{\text{m}}$ ; (b)  $\Delta K = 19 \text{ MPa}\sqrt{\text{m}}$ .

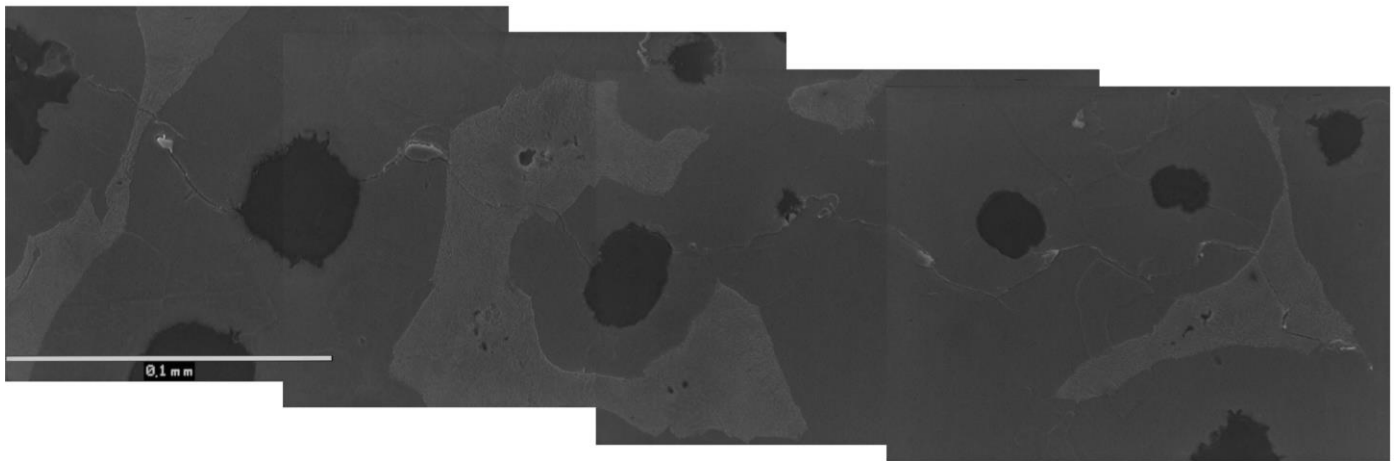


Figure 7: Fatigue crack path: phases influence (crack grows from left to right).  $\Delta K = 17 \text{ MPa}\sqrt{\text{m}}$ .

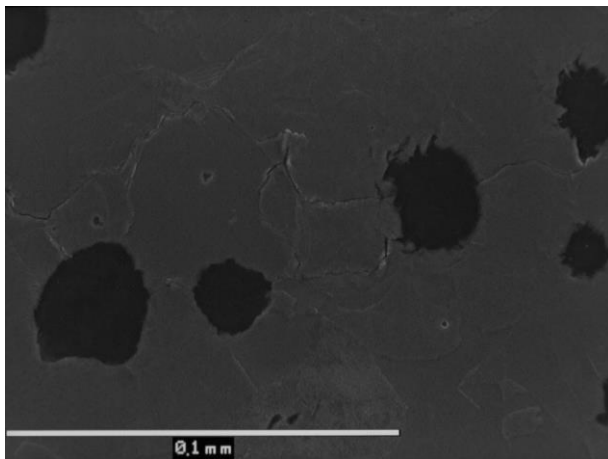


Figure 8: Secondary crack (crack grows from left to right).  $\Delta K = 13 \text{ MPa}\sqrt{\text{m}}$ .

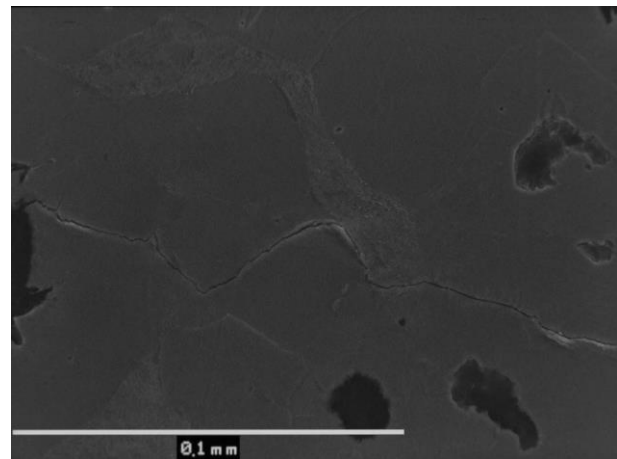


Figure 9: Intergranular crack path crack (crack grows from left to right).  $\Delta K = 14 \text{ MPa}\sqrt{\text{m}}$ .

Higher magnification SEM observations allow to confirm the behaviour described in Fig. 5, with evident crack deviations due to the graphite nodules presence (Fig. 6). In addition, it is possible to observe that, corresponding to the graphite nodules, the main damaging micromechanisms is the debonding between the graphite nodule and the matrix (mainly ferrite, see also Fig. 4), although, seldom, the crack pass through the graphite nodules (Fig. 6b). This behaviour is

completely different with respect to the damaging micromechanisms observed during tensile tests [11, 12], where the mechanical properties gradient inside the graphite nodules plays a key role and secondary cracks inside graphite nodules nucleate and propagate (“onion-like” mechanism).

Considering the crack path in the ferritic-pearlitic matrix, crack mainly propagates transgranularly, with slip bands that emanate from the crack tip (more evident in the ferritic matrix, at least according to the SEM observation). Ferrite-pearlite interfaces influence on crack path is evident in Fig. 7. The intersection between the crack path and the ferrite-pearlite interfaces always implies a crack path direction modification, with a consequent increase of the fracture surface roughness (and of the roughness induced crack closure effect). In addition, both secondary cracks (Fig. 8) and intergranular crack path (Fig. 9) are seldom observed.

Considering the fracture mechanics principles, and, as first approximation, assuming the investigated DCI as an homogeneous and linear elastic material, it is possible to roughly describe the stress state at the crack tip. Fig. 10 [13] shows the different zones ahead the crack tip during a fatigue loading:

- reverse/cyclic plastic zone (orange, rpz): fatigue loading implies a stress hysteresis loop depending upon the stress ratio R and the applied value of  $\Delta K$ .
- monotonic plastic zone (yellow, mpz): plastic deformation occur during monotonic loading and, after that, elastic loading-unloading takes place
- elastic zone (grey, ez): the deformation is completely elastic.

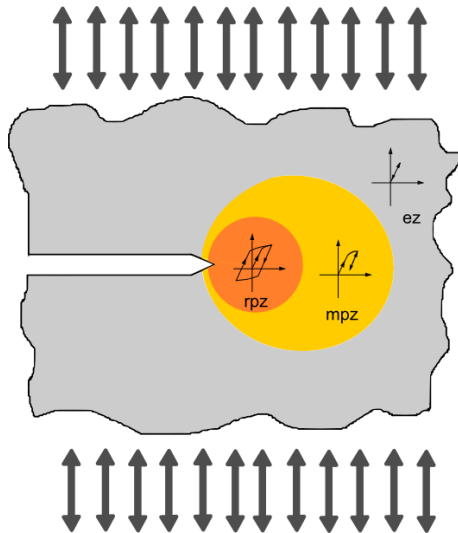


Figure 10: Fatigue crack propagation: rpz (reversed plastic zone); mpz (monotonic plastic zone); ez (elastic zone).

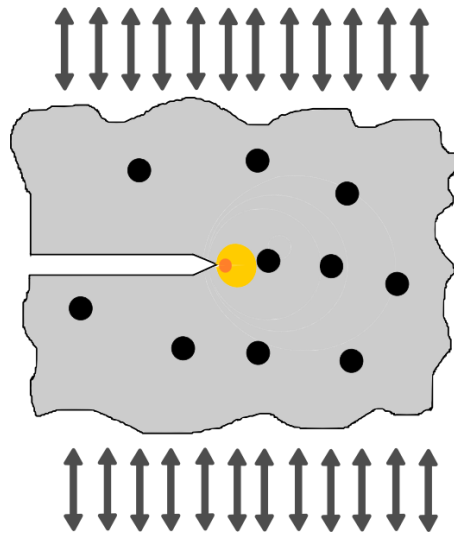


Figure 11: rpz and mpz compared to graphite nodules corresponding to lower  $\Delta K$  values (e.g. 10  $\text{MPa}\sqrt{\text{m}}$ ).

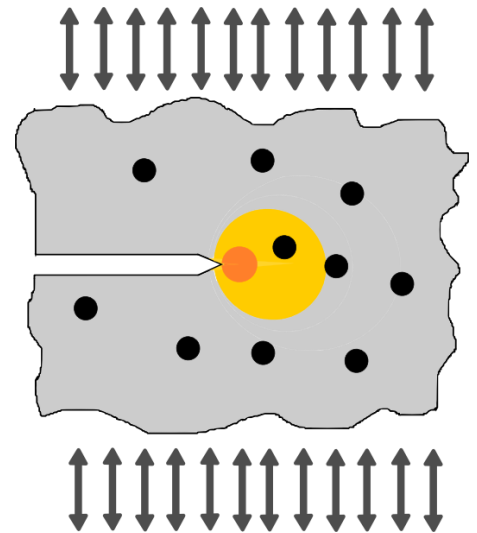


Figure 12: rpz and mpz compared to graphite nodules corresponding to higher  $\Delta K$  values (e.g. 20  $\text{MPa}\sqrt{\text{m}}$ ).

Corresponding to the lateral surface (plane stress conditions):

$$r_y = \frac{1}{2\pi} \left( \frac{K}{\sigma_y} \right)^2 \quad (2)$$

The “reversed” or “cyclic” plastic zone ( $r_{rpz}$ ), the volume which undergoes yielding due to both tensile and compressive stress, is four times lower than the monotonic value corresponding to  $K_{\text{max}}$ . Considering the investigated loading conditions, for  $\Delta K$  values ranging between 10 and 20  $\text{MPa}\sqrt{\text{m}}$ , the corresponding  $r_{rpz}$  values range between about 30 and about 120  $\mu\text{m}$ , or rather between the half and the double of the maximum measured graphite nodules diameters. Instead, considering the matrix,  $r_{rpz}$  values are lower or comparable to the ferrite grains or pearlite colonies diameters. As a consequence, fatigue crack propagation in the investigated ferritic-pearlitic DCI can be analysed with the  $\Delta K$  parameter only as first approximation, being the material non homogenous, at least at the scale of the fatigue damaging processes at the crack tip.

Considering lower  $\Delta K$  values, two conditions are possible:

- graphite nodules free zone (Fig. 10): rpz and mpz are lower than the ferritic grain or pearlitic colonies diameters. Material can be considered as microscopically homogeneous and the propagation is mainly influenced by the metal matrix (e.g., with slip bands in ferritic grains).
- graphite nodules ahead the crack tip (Fig. 11 and 13): mpz interact with the matrix-graphite nodule interface. Considering the nodule ahead the mpz in Fig. 13, the left side is plastically stressed, with the right side that is still elastically stressed. Matrix and graphite nodules different mechanical behaviour implies the activation of the nodule-matrix debonding (Fig. 13b). When crack propagates up to the graphite nodule (Fig. 13c), the debonding can be completely developed and the graphite nodule can only influence the closure effect, according to the mechanism described in Fig. 3 [5].

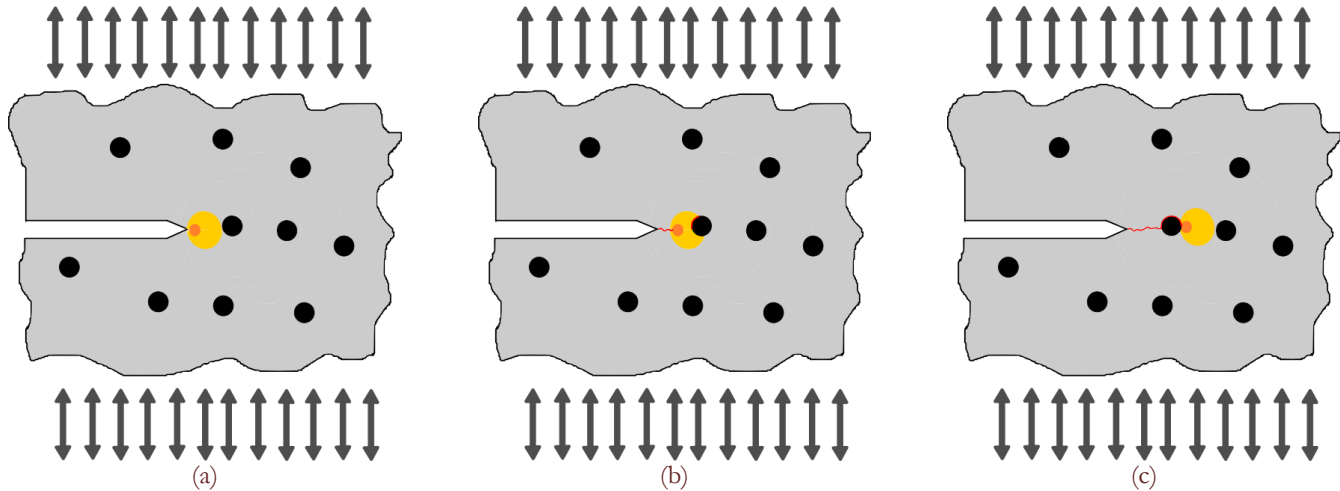


Figure 13: Fatigue crack propagation. Interaction between rpz, mpz and graphite nodules (lower  $\Delta K$  values).

Considering higher  $\Delta K$  values, two conditions are still possible:

- graphite nodules free zone (Fig. 10): rpz and mpz are larger than the ferritic grain or pearlitic colonies diameters. Material can be considered as microscopically homogeneous and as a polycrystalline material.
- graphite nodules ahead the crack tip (Fig. 12 and 14): larger rpz and mpz allows an interaction also with graphite nodules that are not exactly ahead the crack tip. Graphite nodules in the mpz “attract” the crack path due to the influence of their presence on the crack tip stress field, with an increase of the crack path tortuosity and a consequent increase of the fracture surface roughness.

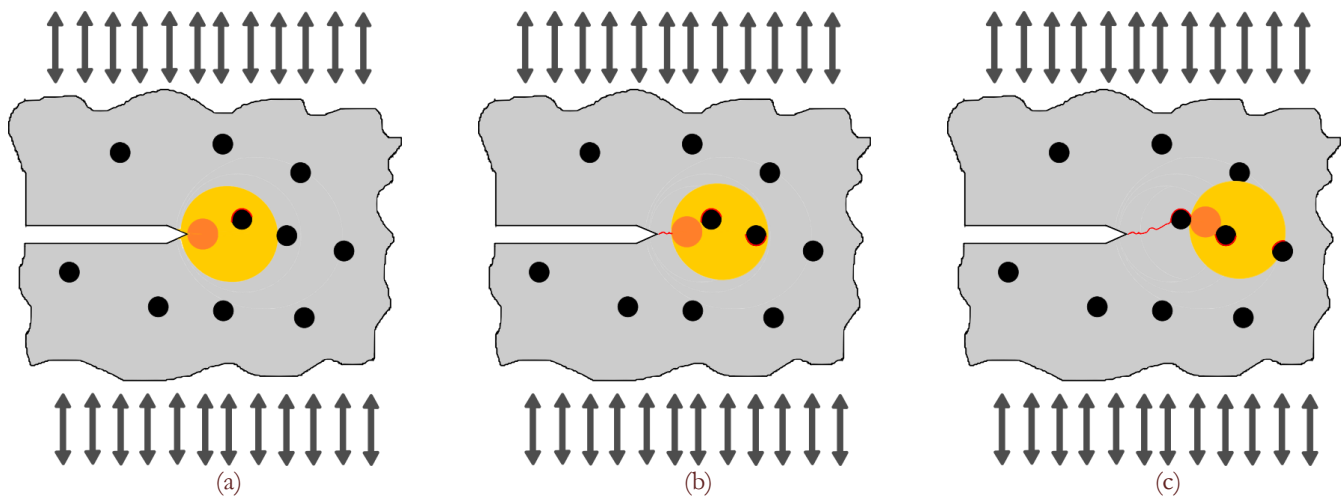


Figure 14: Fatigue crack propagation. Interaction between rpz, mpz and graphite nodules (higher  $\Delta K$  values).

SEM fracture surface analysis confirms this behaviour: corresponding to all the observed graphite nodules, it is possible to observe both not damaged nodules, or voids without graphite residuals (Fig. 15).

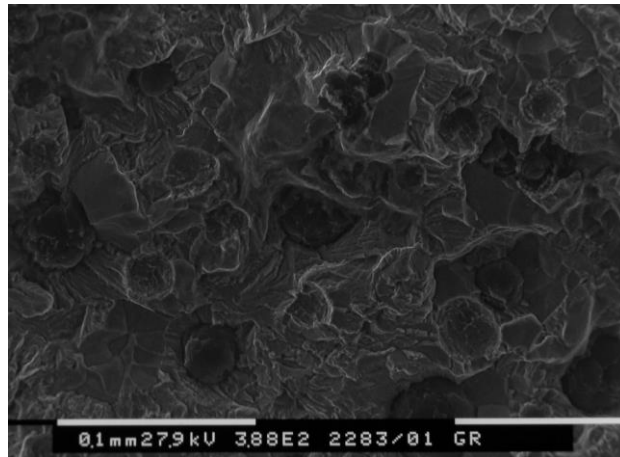


Figure 15: SEM fracture surface analysis ( $\Delta K = 10 \text{ MPa}\sqrt{\text{m}}$ )

## CONCLUSIONS

In this work, fatigue crack propagation micromechanisms in a ferritic-pearlitic DCI have been investigated, focusing on both the graphite nodules role and the crack tip stress condition. Considering as first approximation the DCI as an homogenous material, the analysis of the experimental results allows to summarize the following conclusion:

- The main contribution of the graphite nodules to the damaging micromechanisms is the graphite nodules – matrix debonding. This is due to the interaction of the rpz and mpz with the graphite nodule/matrix interface.
- The increase of the applied  $\Delta K$  implies an increase of the number of graphite nodules that can be embedded in the mpz. As a consequence the increase of the  $\Delta K$  implies a more tortuous crack path with a consequent increase of the crack surface roughness and of the roughness induced crack closure effect.
- If the mpz and rpz are nodule free, the crack propagates generating slip bands at the crack tip, more evident in ferrite grains.
- This propagation micromechanism is compatible with the “spheroid presence induced” crack closure effect described in [5]: also this mechanism becomes more evident with the increase of the applied  $K_{\text{max}}$  (and, as consequence, of the mpz radius).

## REFERENCES

- [1] Jenkins, L.R., Forrest, R.D., Ductile Iron, in Properties and selection: iron, steels and high performance alloys. ASM Handbook, Metal Park (OH) ASM International, 1 (1993) 35-55.
- [2] Canzar, P., Tonkovic, Z., Kodvanj, J., Microstructure influence on fatigue behaviour of nodular cast irons, *Materials Science and engineering A*, 556 (2012) 88-99.
- [3] Labrecque, C., Gagne, M., Review ductile iron: fifty years of continuous development, *Can. Metall. Quart.*, 37 (1998) 343-378.
- [4] [www.advancedcast.com/adi-advantages.htm](http://www.advancedcast.com/adi-advantages.htm) (2015).
- [5] Cavallini, M., Di Bartolomeo, O., Iacoviello, F., Fatigue crack propagation damaging micromechanisms in ductile cast irons, *Engineering Fracture Mechanics*, 75 (2008) 694-704. DOI: 10.1016/j.engfracmech.2007.02.002.
- [6] Cavallini, M., Di Bartolomeo, O., Iacoviello, F., Fatigue damaging micromechanisms in ductile cast irons, In: *Proceedings of International Conference on Fatigue Crack Paths (CP2006)*, Parma, Italy, (2006) 13.
- [7] ASTM Standard test Method for Measurements of fatigue crack growth rates (ASTM E647 - 13ae1). *Annual Book of ASTM Standards*. 0301, American Society for Testing and Materials, (2013).
- [8] Iacoviello, F., Polini, W., Influenza della matrice sulla propagazione di cricche di fatica nelle ghise sferoidali, *La Metall. Ital.*, 7/8 (2000) 31–34.
- [9] Iacoviello, F., Di Cocco, V., Ductile Cast irons: microstructure influence on fatigue crack propagation resistance, *Frat. Ed Integrità Strutt.* 13 (2010) 3–16. DOI: 10.3221/IGF-ESIS.13.01.



- [10] Elber, W., The significance of fatigue crack closure, Damage tolerance in aircraft structures, ASTM STP 486, American Society for Testing and Materials, (1971) 230 – 242.
- [11] Di Cocco, V., Iacoviello, F., Rossi, A., Damaging micromechanisms characterization in a ferritic-pearlitic ductile cast iron, *Frat. Ed Integrità Strutt.*, 8 (2014) 62–67. DOI: 10.3221/IGF-ESIS.30.09
- [12] Di Cocco, V., Iacoviello, F., Rossi, A., Iacoviello, D., Macro and microscopical approach to the damaging micromechanisms analysis in a ferritic ductile cast iron, *Theor. Appl. Fract. Mech.* 69 (2014) 26–33. DOI: 10.1016/j.tafmec.2013.11.003.
- [13] Paul, S. K., Tarafder, S., Cyclic plastic deformation response at fatigue crack tips, *International Journal of Pressure Vessels and Piping* 101, (2013) 81-90. DOI: 10.1016/j.ijpvp.2012.10.007.
- [14] Iacoviello, F., Di Cocco, V., Rossi, A., Cavallini, M., Fatigue crack propagation damaging micromechanisms in pearlitic ductile cast irons, *Fatigue Fract. Eng. Mater. Structures*, 38 (2015) 238–245. DOI: 10.1111/ffe.12215.